Electrochimica Acta 55 (2010) 6907–6916

Contents lists available at ScienceDirect

Electrochimica Acta

journal homepage: www.elsevier.com/locate/electacta

Potential control characteristics of short-chain thiols of thioctic acid and mercaptohexanol self-assembled on gold

Zhiguo Li [a], Tianxing Niu [a], Zhenjiang Zhang [a,b], Shuping Bi [a,*]

[a] School of Chemistry and Chemical Engineering, State Key Laboratory of Coordination Chemistry & Key Laboratory of MOE for Life Science, Nanjing University, Nanjing 210093, China
[b] College of Chemistry, Chemical Engineering and Materials Science, Soochow University, Suzhou 215006, China

ARTICLE INFO

Article history:
Received 13 December 2009
Received in revised form 1 May 2010
Accepted 6 May 2010
Available online 18 June 2010

Keywords:
Thioctic acid
Mercaptohexanol
Potential control
Self-assembled monolayers
Cyclic voltammetry
Electrochemical impedance spectroscopy

ABSTRACT

In this article we systematically investigated self-assembly of short-chain thiols of thioctic acid (TA) and mercaptohexanol (MCH) on gold under potential control, E_{dc} (−0.4, +0.4 and +0.7 V) and compared the results obtained with open circuit potential (E_{OCP}). Effect of E_{dc} on thiol self-assembly was inspected based on the changes in electrochemical parameters including interfacial capacitance (C), phase angle ($\Phi_{1\ Hz}$), current density difference (Δi), charge transfer resistance (R_{ct}) through cyclic voltammetry (*CV*) and electrochemical impedance spectroscopy (*EIS*). Experimental results showed that E_{dc} could not obtain stable short-chain self-assembled monolayers (SAMs) (TA and MCH) in a short time. Both TA and MCH had slow self-assembly dynamics and needed a long time (> 24 h) to achieve adsorption equilibrium. Furthermore, the negative potential E_{dc} (−0.4 V) did not facilitate the ordering of SAMs. The ordering of TA-SAMs was found to be the best when assembled under E_{dc} (+0.4 V), whereas that of MCH-SAMs was almost the same when assembled under either E_{OCP} or E_{dc} (+0.4, +0.7 V). We considered that permeation of ions and water molecules perhaps dominated the slow self-assembly dynamics of short-chain thiols (TA and MCH) under E_{dc} and mutual interaction between adjacent chains of thiols played an important role in the ordering of SAMs.

1. Introduction

Self-assembled monolayers (SAMs) are widely applied in a variety of fields due to their diversity and functionality for interface at the molecular level [1–4]. Processes for the self-assembly of thiols are generally divided into two steps [5]: rapid adsorption and slow ordering. These two different steps are affected by many factors, like surface pretreatment of the gold substrate, potential control, solvent, temperature and the concentration of the thiols used [1,5–29]. Potential control (direct current potential, E_{dc}) has a lot of advantages for the self-assembly of thiols (e.g., accelerating the adsorption dynamics of thiols, improving the quality of SAMs and achieving the controlled self-assembly of thiols) (Table S1, supporting information) [11–28]. Studies on the self-assembly of thiols under E_{dc} are mainly from the aspect of the early adsorption rate of thiols (RSH). In strong alkaline solutions, RSH converts to RS^- due to dissociation of H^+. Positive E_{dc} can accelerate the surface adsorption of RS^- because of electrostatic attraction between RS^- and the electrode [11]. In acidic or neutral solutions, thiols exist as RSH and the early adsorption rate of thiols is determined by either the accumulation or absence of electrons on the electrode surface [25] or the rupture of the S–H bond [12]. Studies also assess the quality of the SAMs created. Researchers have shown that applying positive E_{dc} can accelerate self-assembly of long-chain thiols and provide more ordered SAMs in a shorter time [13–16].

It is important to study the self-assembly of short-chain thiols under E_{dc}, since short-chain thiols with terminal functionalities ($-NH_2$, $-COOH$, $-OH$) have been widely used to combine proteins, antigens, amino acids, polyelectrolytes and DNA through covalent bonds or electrostatic interactions [29–34]. Short-chain thiols are amenable to the preparation of highly sensitive sensors because electron transfer proceeds easily owing to the short distance between the analyte and the working electrode [35,36]. Furthermore, short-chain SAMs are often used to simulate "ion-channels" in biology [30–32]. Macroscopic performances of short-chain SAMs are closely related to their microscopic structures [38], which influence surface chemistry of binding molecules (e.g., protein and enzyme) and molecular recognition properties of sensors based on thiol SAMs [38–43]. It is necessary to obtain more ordered and stable short-chain SAMs in a shorter assembly time to improve efficiency, reproducibility and stability. It has been reported, however, that long time is usually necessary for short-chain thiols to form stable SAMs when assembled under E_{OCP} [44,45]. Additionally, the

* Corresponding author. Tel.: +86 25 83594255; fax: +86 25 83317761.
E-mail address: bisp@nju.edu.cn (S. Bi).

0013-4686/$ – see front matter © 2010 Elsevier Ltd. All rights reserved.
doi:10.1016/j.electacta.2010.05.028

order of short-chain SAMs can be improved through electrochemical methods [28,35,46], but self-assembly of short-chain thiol SAMs under E_{dc} has been studied little until now.

In this article, we study self-assembly of two short-chain thiols, including TA and MCH (Figure S1, supporting information), on gold under E_{dc} (−0.4, +0.4 and +0.7 V) compared to E_{OCP}. Effect of E_{dc} on thiol self-asembly is inspected based on the changes in electrochemical parameters (interfacial capacitance C, phase angle $\Phi_{1\ Hz}$, current density difference Δi, charge transfer resistance R_{ct}) through *CV* and *EIS* for three aspects: (a) self-assembly for short periods of time (30 min) under different E_{dc} to investigate whether E_{dc} can accelerate surface adsorption of short-chain thiols and form more stable SAMs quickly; (b) self-assembly for longer time (24 h) under different E_{dc} to investigate the quality of short-chain SAMs; and (c) self-assembly at different time (from 2 min to 72 h) under the optimal E_{dc} to investigate the adsorption dynamics of short-chain thiols. Possible mechanisms for the effect of E_{dc} on self-assembly of TA and MCH on gold are also discussed.

2. Experimental

2.1. Chemicals and apparatus

DL-thioctic acid (TA; 98%, Alfa), 6-mercapto-1-hexanol (MCH; 97%, Aldrich), anhydrous sodium sulfate (Na_2SO_4; 99%, Alfa), potassium hexacyanoferrate (III) ($K_3Fe(CN)_6$; 99%, Sigma) and ethanol (99.9%, Merck) were of analytical grade and used as received. Double-distilled water was used to prepare the aqueous solutions. Electrochemical measurements were performed on a CHI660 (CH Instruments, USA) electrochemical workstation. Equivalent circuit fitting analysis of *EIS* was obtained using Zsimpwin software. The cell was a three-electrode system with a working electrode of polycrystalline gold (geometric surface area, 0.0314 cm^2, CH Instruments), a counter electrode of platinum and a reference electrode of saturated calomel (SCE). Solutions were degassed with nitrogen for at least 15 min prior to each experiment and a nitrogen atmosphere was maintained over the solutions. The temperature was kept at 25 ± 1 °C over the course of the experiment with a CS-501SP super digital thermostat bath (Huida Experimental Equipment Ltd., Chongqing, China).

2.2. Pretreatment of gold electrodes

Polycrystalline gold electrodes were hand-polished with microcloth pads and alumina slurries of decreasing particle size (1.0, 0.3 and 0.05 μm), then dipped into newly prepared piranha solution [24] (concentrated H_2SO_4:30% H_2O_2 = 3:1, v:v) for 2 min. The gold electrodes were then sonicated in double-distilled water for 15 min and electrochemically polished in N_2-purged 0.5 M H_2SO_4 solution from −0.4 to +1.5 V at 0.1 V s^{-1} until reproducible voltammograms were obtained. Following this, the electrodes were rinsed with double-distilled water and ethanol, then blown dry with 99.999% pure nitrogen. The real surface area of the gold electrodes were determined by integrating the charge of reduction peak for gold, assuming a value of 400 μC cm^{-2} for a monolayer of chemisorbed oxygen on polycrystalline gold [35]. The roughness factor of the gold electrode was found to be 1.5 ± 0.2.

2.3. Preparation of SAMs

By experiment (Figure S2, supporting information), it was concluded that the charging current zone of gold in 0.1 M $LiClO_4$ ethanolic solution was from −1.2 to 0.7 V. In the presence of TA or MCH, the charging current zone was observed to change. For TA-SAMs, the zone was from −0.6 to 0.9 V, and for MCH-SAMs, −0.6 to 1.0 V. Open circuit potential (*OCP*) showed that E_{OCP} of bare gold in 0.1 M $LiClO_4$ ethanolic solution was located at 0.25 ± 0.06 V by experimental determination, in accordance with Lennox's results [14]. When the gold electrodes were dipped into TA or MCH ethanolic solution for assembly, E_{OCP} decreased abruptly (Figure S3, supporting information), consistent with the abrupt change of E_{OCP} reported for other thiols [14,25].

E_{OCP} for self-assembly: Following pretreatment, the gold electrodes were immersed in fresh 1 mM TA or MCH ethanolic solutions under E_{OCP} for self-assembly.

Potential control for self-assembly [13]: The gold electrodes were first immersed in 1 mM TA or MCH in 0.1 M $LiClO_4$ ethanolic solutions for assembly under E_{dc} (−0.4, +0.4 or +0.7 V). When the assembly time was terminated, the gold electrodes were quickly withdrawn from the cell and rinsed with ethanol and double-distilled water. After this, the electrodes were put into the electrochemical cell for experimentation.

Analysis of TA-SAMs and MCH-SAMs assembled under E_{dc} (−0.4, +0.4 or +0.7 V) and E_{OCP} values for 30 min or 24 h were performed in triplicate (n = 3), whereas the dynamic experiments on TA or MCH self-assembly from 2 min to 72 h under the optimal potential or E_{OCP} was from only one measurement.

2.4. Electrochemical characterization

The electrochemical characteristics of SAMs (TA and MCH) were investigated based on the analysis of electrochemical parameters (C, $\Phi_{1\ Hz}$, Δi and R_{ct}) by *CV* and *EIS* (Scheme S1, supporting information).

2.4.1. CV measurements

C was measured from *CV* performed from −200 to +200 mV in 0.1 M Na_2SO_4 solution at different scan rates, v (0.1, 1, 5, 50 V s^{-1}), based on the relationship $C = i/2vA$, where i was the summed current (μA) from the positive and negative scan directions at 0 mV, v was the scan rate (V s^{-1}) and A was the real area of the gold electrodes (cm^2) [31,47,48]. Δi was obtained from *CV* experiments performed in an aqueous solution of 2 mM $K_3Fe(CN)_6$ and 0.1 M Na_2SO_4 with a scan zone from −0.2 to +0.5 V at a rate of 0.1 V s^{-1}. Current density differences for $Fe(CN)_6^{3-}$ at −0.2 V and +0.5 V ($\Delta i = \left| i_{-0.2V} - i_{+0.5V} \right|$) were used to investigate the blocking characteristics of the SAMs (when *CV* of $Fe(CN)_6^{3-}$ gave redox peaks, Δi was the difference of the redox peak current density) [6,8–10].

2.4.2. EIS measurements

The magnitude of phase angle in the low-frequency zone showed the extent of ion permeation through the SAMs and was used to evaluate the tightness of the SAMs [49–53]. The bigger the phase angle was, the tighter were the formed SAMs. The phase angle at 1 Hz ($\Phi_{1\ Hz}$) was found to be suitable for evaluating the tightness of SAMs [51], with $\Phi_{1\ Hz}$ obtained by *EIS* measurement at 0 V in 0.1 M Na_2SO_4 blank solution with a frequency range from 0.1 Hz to 10^5 Hz and a 5 mV amplitude. *EIS* measurements were also carried out in an aqueous solution of 2 mM $K_3Fe(CN)_6$ and 0.1 M Na_2SO_4 in a frequency range of 0.1 Hz to 10^5 Hz with a 5 mV amplitude. The potential in these measurements was fixed at the formal potential, $E^{o'}$ (0.18 V). Plots of *EIS* were simulated from a Randle equivalent circuit (*RQRW*) (Figure S4, supporting information) comprising a parallel combination of constant phase elements (*CPE*), represented by Q, and a faradaic impedance Z_f, in series with the uncompensated solution resistance R_s. The faradaic impedance (Z_f) was a series combination of the charge transfer resistance (R_{ct}) and the Warburg impedance (W) [54].

3. Results and discussion

3.1. Self-assembly of TA and MCH on gold for a short time (30 min) under different E_{dc}

We investigated the electrochemical characteristics of SAMs (TA and MCH) assembled for a short time (30 min) under different E_{dc} by *CV* and *EIS* (Figure 1 and Table 1). Figure 1 (A, B, C and D) shows the *CV* and *EIS* plots for TA-SAMs. Electrochemical parameters (C, Δi, $\Phi_{1\ Hz}$ and R_{ct}) of SAMs were found to be independent of E_{dc}. C decreased gradually with increasing scan rate (v) and $\Phi_{1\ Hz}$ was much smaller than the phase angle of 88° for the ion insulator [51–53]. These reflected typical ion permeations previously found for SAMs [6–10,51–53]. From these data, TA-SAMs obviously impeded the electron transfer of $Fe(CN)_6^{3-}$ with a Δi value of $263 \pm 47\ \mu A\,cm^{-2}$ and a R_{ct} of $1.2 \pm 0.7 \times 10^3\ \Omega\,cm^2$.

Figure 1 (A', B', C' and D') shows the *CV* and *EIS* plots for MCH-SAMs. Similarly, C, Δi, $\Phi_{1\ Hz}$ and R_{ct} of these SAMs were independent of the value of E_{dc} (Table 1). MCH-SAMs showed poor blocking of $Fe(CN)_6^{3-}$ with a Δi of $447 \pm 40\ \mu A\,cm^{-2}$ and a R_{ct} of $0.9 \pm 0.6 \times 10^2\ \Omega\,cm^2$.

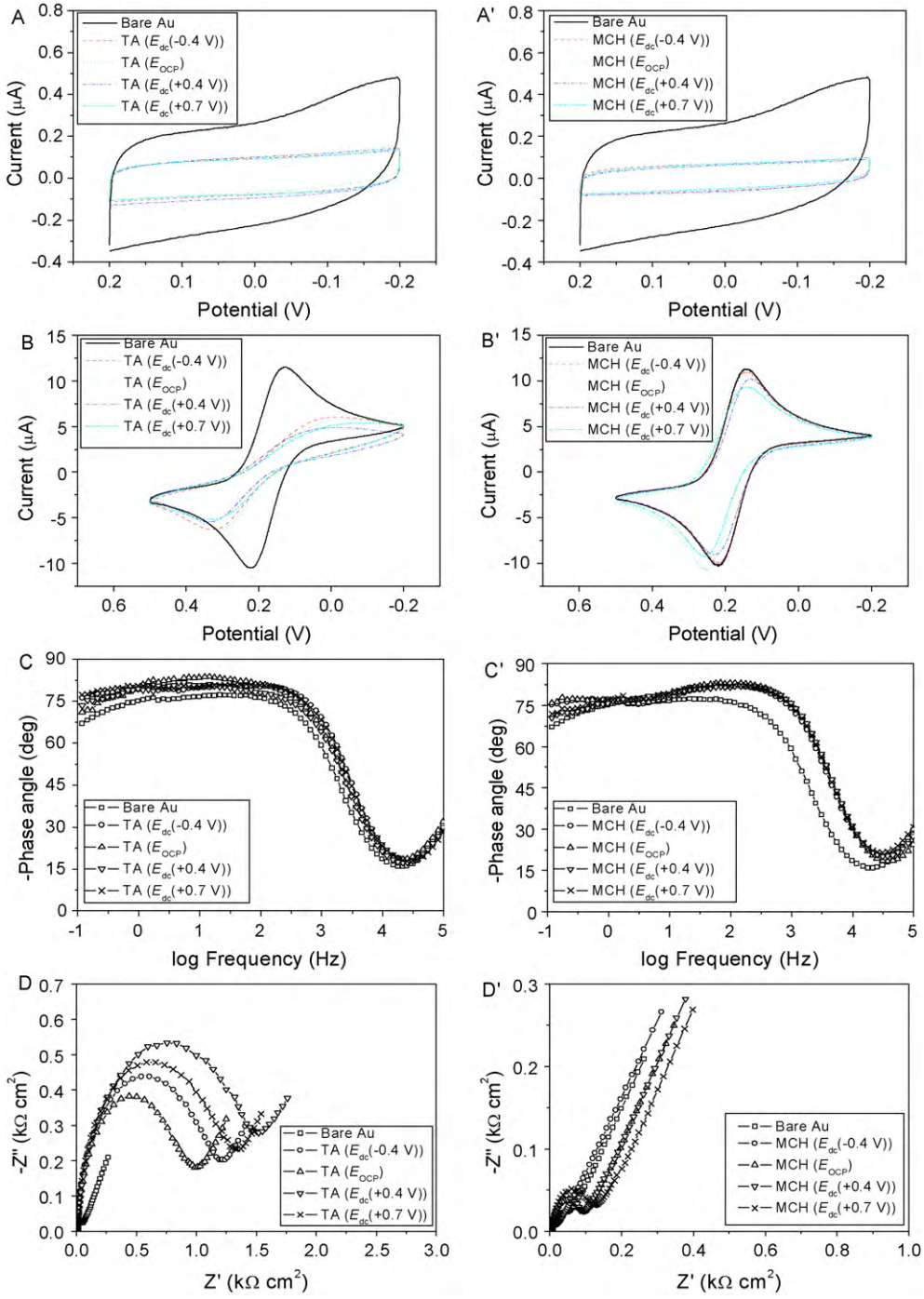

Fig. 1. Characteristics of TA-SAMs and MCH-SAMs assembled for 30 min under different E_{dc}.
(1) *CV* of bare Au and TA-SAMs or MCH-SAMs in a 0.1 M Na_2SO_4 solution (A and A') and a solution of 2 mM $Fe(CN)_6^{3-}$ and 0.1 M Na_2SO_4 (B and B') at 0.1 V s^{-1}.
(2) *EIS* of bare Au and TA-SAMs or MCH-SAMs in a 0.1 M Na_2SO_4 solution (C and C') and a solution of 2 mM $Fe(CN)_6^{3-}$ and 0.1 M Na_2SO_4 (D and D').

Table 1
Interfacial parameters of TA-SAMs and MCH-SAMs assembled under different E_{dc} values.

SAMs	E_{dc} (V)	Assembly time	Ion permeability					$Fe(CN)_6^{3-}$ electron transfer	
			CV				*EIS*	*CV*	*EIS*
			C ($\mu F\,cm^{-2}$)				$\Phi_{1\ Hz}$ (°)	Δi ($\mu A\,cm^{-2}$)	R_{ct} ($\Omega\,cm^2$)
			0.1 V s^{-1}	1 V s^{-1}	5 V s^{-1}	50 V s^{-1}			
TA	−0.4	30 min	19.9 ± 1.3	14.3 ± 0.2	11.6 ± 1.6	9.0 ± 0.8	79 ± 2	318 ± 62	$(0.7 \pm 0.4) \times 10^3$
	E_{ocp}		17.9 ± 1.5	12.7 ± 2.0	10.0 ± 2.2	7.9 ± 2.0	77 ± 3	251 ± 16	$(1.5 \pm 1.1) \times 10^3$
	+0.4		19.8 ± 1.3	14.2 ± 2.2	11.5 ± 2.2	8.5 ± 1.8	78 ± 3	230 ± 20	$(1.5 \pm 0.5) \times 10^3$
	+0.7		18.6 ± 2.6	13.8 ± 1.6	11.3 ± 2.0	8.7 ± 1.7	80 ± 1	254 ± 34	$(1.2 \pm 0.7) \times 10^3$
	−0.4	24 h	17.8 ± 1.4	13.7 ± 2.2	11.6 ± 2.5	9.0 ± 2.0	81 ± 2	166 ± 25	$(7.7 \pm 1.8) \times 10^3$
	E_{ocp}		14.5 ± 1.5	12.2 ± 0.9	10.9 ± 0.7	9.0 ± 0.5	84 ± 1	88 ± 34	$(3.9 \pm 1.2) \times 10^4$
	+0.4		13.8 ± 0.2	11.2 ± 0.7	9.5 ± 1.1	6.6 ± 0.9	83 ± 1	34 ± 14	$(1.8 \pm 1.5) \times 10^5$
	+0.7		17.1 ± 1.4	13.9 ± 1.6	11.4 ± 1.6	9.1 ± 1.5	83 ± 1	122 ± 11	$(1.7 \pm 0.1) \times 10^4$
	E_{ocp}	2 min	25.2	18.5	12.9	7.7	75	331	3.6×10^2
		10 min	23.3	16.0	12.0	9.0	75	315	6.5×10^2
		1 h	16.7	12.7	10.5	8.0	80	197	5.8×10^3
		10 h	14.0	11.6	10.0	7.5	82	227	4.0×10^3
		40 h	15.5	13.3	12.4	9.6	84	65	6.0×10^4
		72 h	15.2	12.8	11.3	9.4	85	52	3.9×10^4
	+0.4	2 min	23.7	15.4	10.1	6.1	73	348	3.8×10^2
		10 min	21.4	15.9	12.3	8.9	78	225	1.1×10^3
		1 h	17.2	13.2	11.3	8.3	81	202	5.4×10^3
		10 h	16.5	13.8	11.4	8.2	83	87	3.7×10^4
		40 h	16.7	14.5	12.3	9.1	85	34	2.0×10^5
		72 h	14.0	11.9	11.2	9.1	84	16	3.0×10^5
	Ref.	—	—	—	11.0 ± 2.5[a]	—	—	—	4.1×10^4 [b]
MCH	−0.4	30 min	14.2 ± 0.7	9.8 ± 0.2	7.9 ± 0.6	6.3 ± 0.6	78 ± 1	447 ± 3	$(0.5 \pm 0.2) \times 10^2$
	E_{ocp}		12.8 ± 3.3	9.1 ± 1.4	7.4 ± 1.1	5.8 ± 0.6	78 ± 3	490 ± 36	$(0.8 \pm 0.7) \times 10^2$
	+0.4		14.6 ± 2.7	9.4 ± 1.8	7.2 ± 1.4	5.6 ± 1.0	75 ± 1	438 ± 38	$(1.5 \pm 0.7) \times 10^2$
	+0.7		13.0 ± 0.7	9.0 ± 0.6	7.0 ± 0.7	5.7 ± 0.7	78 ± 2	415 ± 41	$(0.9 \pm 0.7) \times 10^2$
	−0.4	24 h	13.6 ± 0.3	11.1 ± 1.8	9.1 ± 0.9	6.4 ± 0.6	80 ± 1	340 ± 5	$(2.6 \pm 0.4) \times 10^2$
	E_{ocp}		9.2 ± 1.5	7.9 ± 1.4	7.0 ± 1.2	5.8 ± 0.8	84 ± 2	436 ± 57	$(1.6 \pm 1.2) \times 10^2$
	+0.4		8.8 ± 3.0	7.1 ± 2.3	6.4 ± 1.6	5.4 ± 0.6	84 ± 2	448 ± 91	$(2.4 \pm 2.1) \times 10^2$
	+0.7		10.4 ± 2.0	7.7 ± 0.2	6.8 ± 0.3	5.4 ± 0.6	81 ± 3	385 ± 39	$(2.3 \pm 0.4) \times 10^2$
	E_{ocp}	2 min	16.6	11.2	8.2	6.1	75	450	1.3×10^2
		10 h	12.4	9.8	8.3	6.4	81	503	0.9×10^2
		40 h	7.8	6.2	5.7	4.8	83	443	1.2×10^2
		72 h	7.6	6.7	6.1	5.4	85	387	3.1×10^2
	Ref.	—	—	—	—	3.7[c]	—	—	—

(a) TA-SAMs assembled in 0.1% thiol-containing ethanol solution for time >24 h [47,48]. (b) van Bennekom et al. reported the R_{ct} of 2 mM $Fe(CN)_6^{3-/4-}$ with TA-SAMs in 0.1 M sodium phosphate buffer solution (PBS, pH = 7.4); TA-SAMs were assembled at E_{dc} (+0.2 V) for 60 h in 50 mM TA in 0.1 M PBS [56]. (c) MCH-SAMs assembled in saturated MCH aqueous solution for 30 min [55]. (d) Parameters of TA-SAMs and MCH-SAMs assembled under different E_{dc} for 30 min or 24 h were the average values of triplicate measurements (n = 3) with relative standard deviation (RSD). Parameters of TA-SAMs and MCH-SAMs assembled under E_{ocp} or E_{dc} (+0.4 V) for different time (from 2 min to 72 h) were from one measurement.

3.2. Self-assembly of TA and MCH on gold for a long time (24 h) under different E_{dc} values

Because the electrochemical characteristics of SAMs (TA or MCH) assembled for 30 min under different E_{dc} were almost the same, we studied the self-assembly of TA and MCH on gold under different E_{dc} values over a long period of time (24 h) (Figure 2 and Table 1).

Figure 2 (A, B, C and D) shows the *CV* and *EIS* plots for TA-SAMs. The C (especially the C values calculated at lower v) of SAMs formed under E_{dc} values of −0.4 or +0.7 V was found to be larger than under E_{OCP} or E_{dc} value of +0.4 V which reflected the poorer ordering of SAMs formed under E_{dc} values of −0.4 or +0.7 V. Cheng et al. obtained a C value of $11.0 \pm 2.5\ \mu F\,cm^{-2}$ (calculated at $v = 5.12\ V\,s^{-1}$) for TA-SAMs assembled in thiol-containing ethanol solution under E_{OCP}, which was in accordance with our experimental value [47,48]. TA-SAMs formed under E_{dc} (+0.4 V) impeded electron transfer of $Fe(CN)_6^{3-}$ to the largest extent ($\Delta i = 34 \pm 14\ \mu A\,cm^{-2}$), whereas SAMs formed under a E_{dc} value of −0.4 V showed the poorest blocking of $Fe(CN)_6^{3-}$ with a Δi of $166 \pm 25\ \mu A\,cm^{-2}$ (Figure 2B). $\Phi_{1\ Hz}$ did not display an obvious difference, but was much larger than values obtained for 30 min assembly (Figure 2C). The R_{ct} of $Fe(CN)_6^{3-}$ was the largest at $1.8 \pm 1.5 \times 10^5\ \Omega\,cm^2$ for SAMs formed under a E_{dc} voltage of +0.4 V, while the smallest $7.7 \pm 1.8 \times 10^3\ \Omega\,cm^2$ was obtained for an E_{dc} equal to −0.4 V (Figure 2D).

Figure 2 (A', B', C' and D') illustrates the *CV* and *EIS* plots for MCH-SAMs. SAMs formed under E_{dc} values of −0.4 V were found to be worse than at E_{OCP} or E_{dc} of +0.4 or +0.7 V by comparing the C value (Figure 2A' and Table 1). Furthermore, the C of MCH-SAMs was almost independent of E_{OCP} and E_{dc} at either +0.4 or +0.7 V. MCH-SAMs demonstrated poor blocking of $Fe(CN)_6^{3-}$ electron transfer with a Δi of $402 \pm 66\ \mu A\,cm^{-2}$ (Figure 2B' and Table 1). $\Phi_{1\ Hz}$ of SAMs formed under different E_{dc} values was similar and much larger than that for the 30 min assembly (Figure 2C'). The R_{ct} of $Fe(CN)_6^{3-}$ was found to be $2.2 \pm 1.1 \times 10^2\ \Omega\,cm^2$ (Figure 2D' and Table 1).

3.3. Self-assembly of TA and MCH on gold for different time (from 2 min to 72 h) under the optimal E_{dc}

We assembled TA and MCH on gold for different assembly time (from 2 min to 72 h) to investigate the adsorption dynamics of thiols. Because the ordering of TA-SAMs formed under an E_{dc} value of +0.4 V was determined to be best, we compared the self-assembly dynamics of TA on gold at E_{dc} +0.4 V and at E_{OCP}. From this study, we found that the ordering of MCH-SAMs was worse when assembled under a E_{dc} of −0.4 V and almost the same when assembled

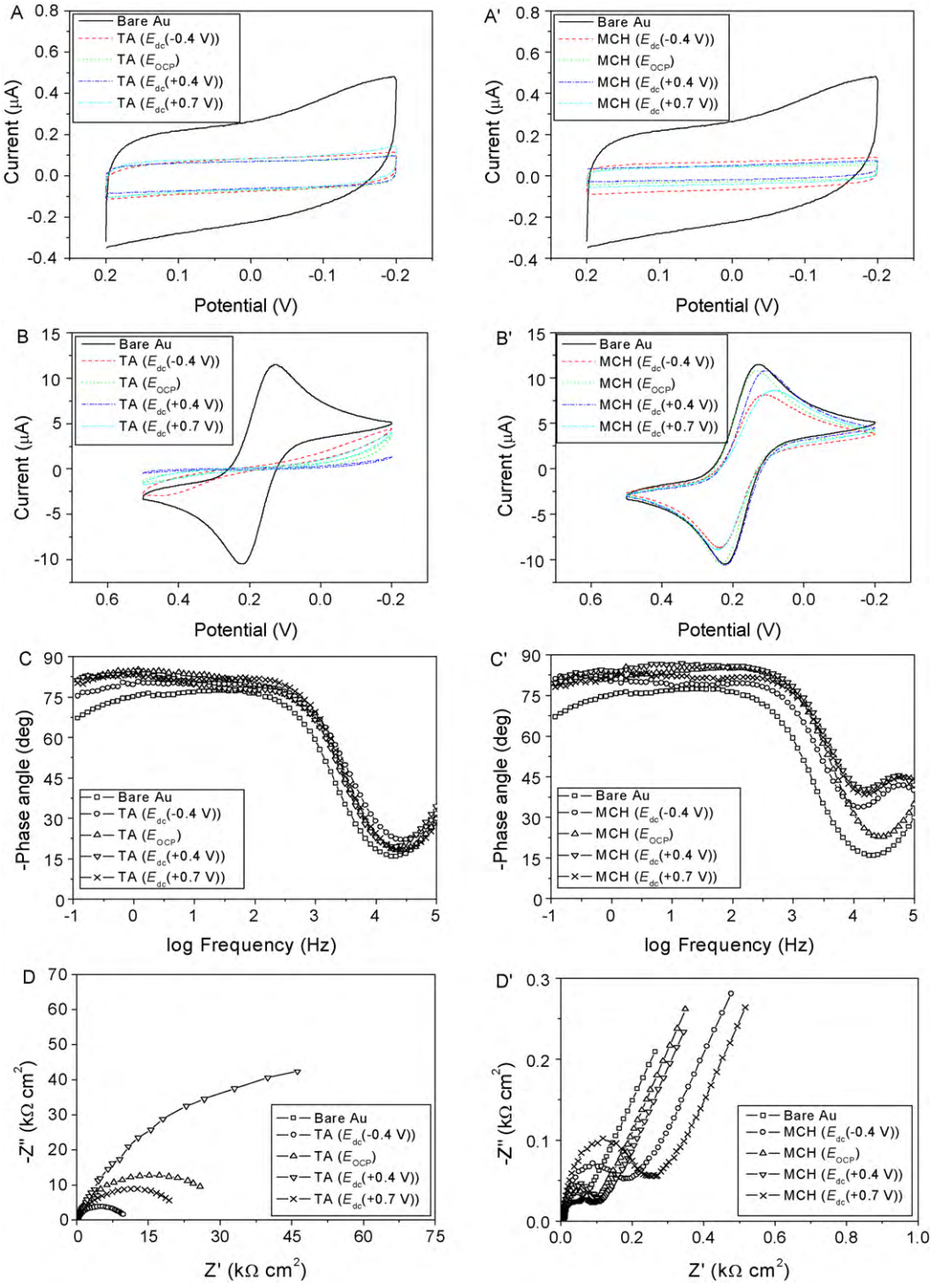

Fig. 2. Characteristics of TA-SAMs and MCH-SAMs assembled for 24 h under different E_{dc}.
(1) *CV* of bare Au and TA-SAMs or MCH-SAMs in a 0.1 M Na_2SO_4 solution (A and A') and a solution of 2 mM $Fe(CN)_6^{3-}$ and 0.1 M Na_2SO_4 (B and B') at 0.1 V s^{-1}.
(2) *EIS* of bare Au and TA-SAMs or MCH-SAMs in a 0.1 M Na_2SO_4 solution (C and C') and a solution of 2 mM $Fe(CN)_6^{3-}$ and 0.1 M Na_2SO_4 (D and D').

under E_{OCP} and E_{dc} of +0.4 or +0.7 V. We therefore only investigated the self-assembly dynamics of MCH on gold under E_{OCP}. The *CV* and *EIS* plots are shown in Figure 3 and the correlative plots of C, $\Phi_{1\ Hz}$, Δi and R_{ct} (Table 1) with self-assembly time are shown in Figure 4.

For TA-SAMs, C calculated at lower v (0.1 V s^{-1}) clearly decreased with increasing time (Figure 4A). However, C calculated at higher v (5 or 50 V s^{-1}) was almost constant (Table 1). This indicated that C obtained at lower v was more sensitive to the structural characteristics of the SAMs. When time for assembly was longer than 10 h, C became stable (Figure 4A). For the same assembly time, the C of TA-SAMs assembled under E_{dc} of +0.4 V was almost the same as that under E_{OCP}. Thavarungkul [57] observed that TA was completely assembled on gold after 12 h by comparing the reductive charge of electroadsoption of oxygen on TA-SAMs and bare gold, consistent with our experimental results. Furthermore, the Δi of $Fe(CN)_6^{3-}$ decreased gradually with increasing time (Figure 4B). When assembled under E_{dc} of +0.4 V and E_{OCP} for short time ($\leq$ 1 h), Δi was

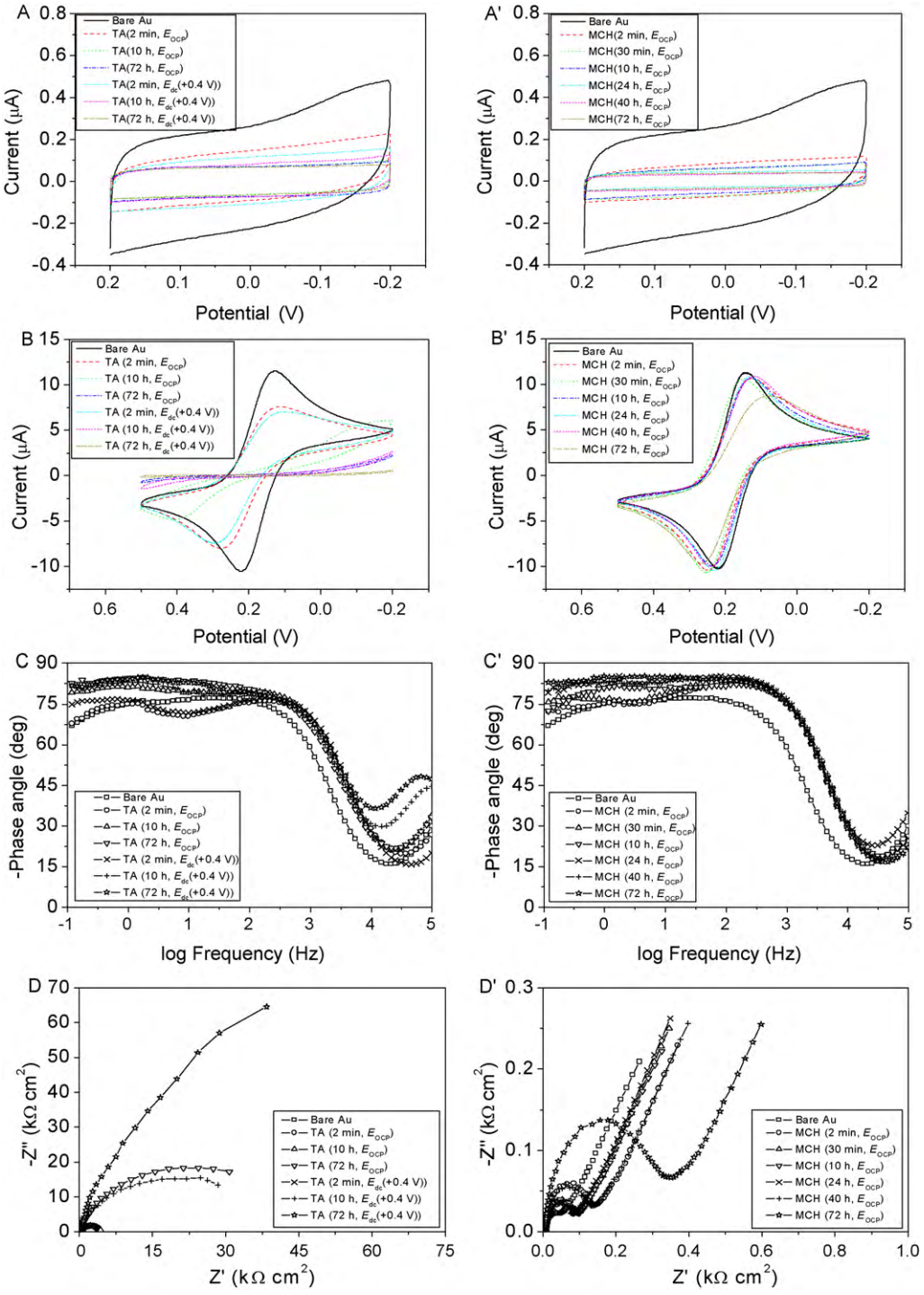

Fig. 3. Characteristics of TA-SAMs and MCH-SAMs assembled for different time (from 2 min to 72 h) under E_{dc} (+0.4 V) or E_{OCP}.
(1) *CV* of bare Au and TA-SAMs or MCH-SAMs in a 0.1 M Na_2SO_4 solution (A and A') and a solution of 2 mM $Fe(CN)_6^{3-}$ and 0.1 M Na_2SO_4 (B and B') at 0.1 V s^{-1}.
(2) *EIS* of bare Au and TA-SAMs or MCH-SAMs in a 0.1 M Na_2SO_4 solution (C and C') and a solution of 2 mM $Fe(CN)_6^{3-}$ and 0.1 M Na_2SO_4 (D and D').

almost the same, but when assembled for longer time ($\geq$ 10 h), SAMs formed under E_{dc} of +0.4 V effectively blocked electron transfer in $Fe(CN)_6^{3-}$. Compared with the electrochemical response of $Fe(CN)_6^{3-}$ on bare Au, Δi was reduced by 97% for TA-SAMs formed under E_{dc} of +0.4 V, but only by 91% under E_{OCP} for 72 h assembly (Table 1). $\Phi_{1\ Hz}$ became larger with the increase in time (Fig. 4A), with $\Phi_{1\ Hz}$ increasing from 74° for 2 min of assembly to 85° for 72 h of assembly. Also, $\Phi_{1\ Hz}$ was independent of E_{dc} (+0.4 V) and E_{OCP} for the same assembly time. R_{ct} of $Fe(CN)_6^{3-}$ was almost the same when assembled under E_{dc} (+0.4 V) and E_{OCP} for a short time ($\leq$ 1 h), while R_{ct} was much larger for TA-SAMs assembled under E_{dc} (+0.4 V) for a long time ($\geq$ 10 h), which then became constant beyond 24 h (Figure 4B).

For MCH-SAMs, C calculated at lower ν (0.1 V s^{-1}) was observed to gradually decrease (Figure 4A). When assembled under E_{OCP} for time beyond 24 h, C became stable. In the same series, Δi was almost constant for the different assembly time (Figure 4B). Additionally, $\Phi_{1\ Hz}$ became larger with the longer time and became stable for time beyond 24 h (Figure 4A). R_{ct} values were almost constant for the different assembly time (Figure 4B).

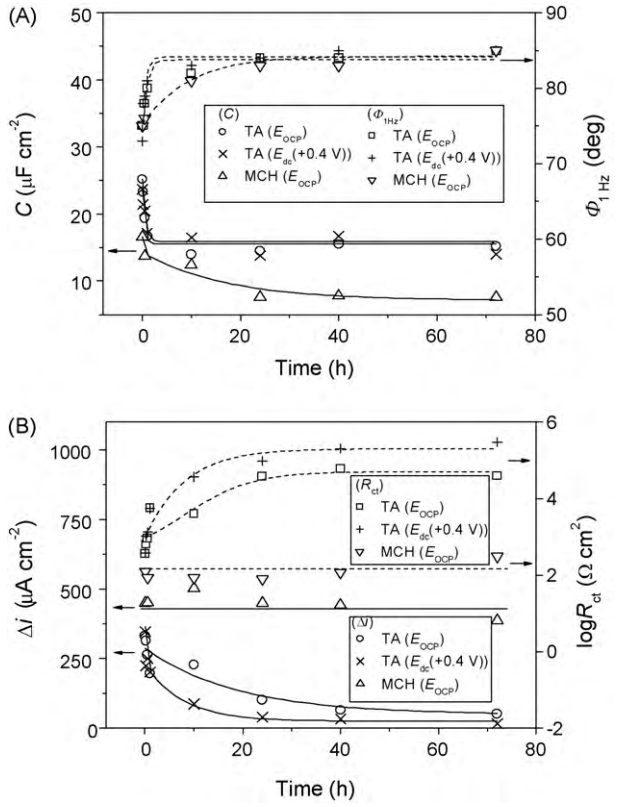

Fig. 4. Relationship of electrochemical parameters: A, C (calculated at $v = 0.1\ V\ s^{-1}$) and $\Phi_{1\ Hz}$; B, Δi and R_{ct} of TA-SAMs and MCH-SAMs assembled under E_{dc} (+0.4 V) or E_{OCP} with self-assembly time from 2 min to 72 h.

3.4. Relationships of $C \sim v$, $\Phi_{1\ Hz} \sim C$ and $\Delta i \sim \log R_{ct}$ for TA-SAMs and MCH-SAMs

C, $\Phi_{1\ Hz}$, Δi and R_{ct} had different meanings in the characterization of the structure of SAMs [58–62]. C showed the average distribution of ions and water in SAMs [58], while $\Phi_{1\ Hz}$ reflected the magnitude of ion permeation in SAMs [51–53]. Δi and R_{ct}, on the other hand, were highly sensitive to structural defects in the SAMs [59–62].

Figure 5A shows the plots of C and v. The C of SAMs decreased with an increase in v, which was related to ion permeation in the SAMs. The relationships of $\Phi_{1\ Hz}$ with C obtained at $0.1\ V\ s^{-1}$ and of Δi with $\log R_{ct}$ were linear with the equations listed below (Figure 5B and Figure 5C).

For TA,

$$\Phi_{1\ Hz}(^\circ) = 96.3 - 0.883C(\mu F\ cm^{-2})(R^2 = 0.863)$$
$$\log R_{ct}\ (\Omega\ cm^2) = 5.23 - 7.85 \times 10^{-3}\Delta i(\mu A\ cm^{-2})(R^2 = 0.972)$$

For MCH,

$$\Phi_{1Hz}(^\circ) = 92.8 - 1.09C(\mu F\ cm^{-2})(R^2 = 0.886)$$
$$\log R_{ct}(\Omega\ cm^2) = 3.93 - 4.06 \times 10^{-3}\ \Delta i\ (\mu A\ cm^{-2})(R^2 = 0.846)$$

For the same thiols, C obtained at lower v (0.1 or $1\ V\ s^{-1}$) had a large variation, whereas C calculated for higher v (5 or $50\ V\ s^{-1}$) was almost constant (Figure 5A). Considering the linear relationship of C ($0.1\ V\ s^{-1}$) with $\Phi_{1\ Hz}$ (Figure 5B), this indicated that C obtained at lower v had similar meaning to $\Phi_{1\ Hz}$ (at lower frequencies) and could conveniently and roughly characterize ion permeability in SAMs. The $C \sim v$ plots for C_{12}SH-SAMs reported [7,9] by us also proved the above conclusion.

For different thiols, $\Phi_{1\ Hz}$ and C were not correlative and SAMs with bigger C did not necessarily indicate smaller $\Phi_{1\ Hz}$. Experimental results ($\Phi_{1\ Hz}$ with C) of $HS(CH_2)_{n-1}CH_3$-SAMs (n = 8, 10, 12, 16) reported by Lennox et al. [52] also agreed with the above conclusion. The reason for this phenomenon was that $\Phi_{1\ Hz}$ only reflected ion permeation in SAMs [51–53], whereas C was related to the magnitude of both the average dielectric constant and the dielectric thickness in the interfacial region of the SAMs [47,48].

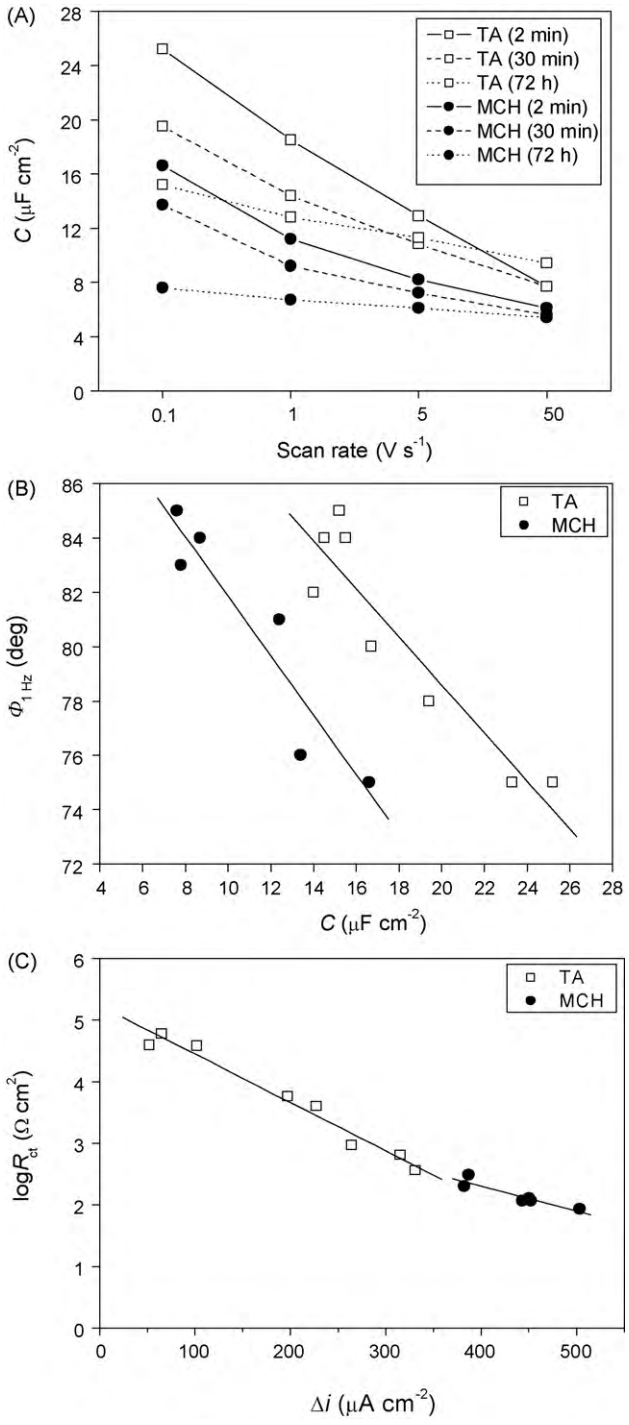

Fig. 5. The plots of (A) C versus scan rate v, (B) $\Phi_{1\ Hz}$ versus C and (C) $\log R_{ct}$ versus Δi for SAMs (TA and MCH). Data in Figure 5 were from the experiments of TA-SAMs and MCH-SAMs assembled under E_{OCP} from 2 min to 72 h in a thiol-containing ethanol solution.

Δi and R_{ct} were more sensitive to the surface structure of the TA-SAMs than the MCH-SAMs (Figure 5C). Because of the electrostatic repulsion between the terminal–COO^- groups of TA ($pK_a = 6.5$) and

$Fe(CN)_6^{3-}$ [63], $Fe(CN)_6^{3-}$ did not permeate well into the SAMs and arrive at the gold surface. The magnitude of Δi and R_{ct} reflected these collapsed sites in the TA-SAMs [59] and the surface arrangement of terminal–COO^- groups. Therefore, subtle differences in structural characteristics of TA-SAMs could be discerned.

For MCH-SAMs, Δi and R_{ct} were almost independent of E_{dc}. Obvious redox peaks of $Fe(CN)_6^{3-}$ appeared showing that $Fe(CN)_6^{3-}$ could diffuse close to the gold surface and react due to the lack of electrostatic repulsion (–OH, $pK_a > 12$) [64] or defective surface structure in MCH-SAMs. The magnitude of Δi and R_{ct} were found to reflect the defects (pinholes) in the MCH-SAMs. Diffusive layers of $Fe(CN)_6^{3-}$ redox reactions at defects could overlap, leading to the almost constant Δi and R_{ct} measurements. The same electrochemical response of $Fe(CN)_6^{3-}$ on TA-SAMs as that on a bare Au surface in a 0.1 M $HClO_4$ solution [47,48] also reflected the overlap of diffusive layers.

3.5. Discussion of the possible mechanism for the effect of E_{dc} on the self-assembly of short-chain thiols (TA and MCH) on gold

By compiling all the data obtained from our experiments, we concluded that: (a) applying E_{dc} could not form stable SAMs with short (30 min) assembly time with the electrochemical characteristics of SAMs being almost independent of E_{dc} in the case studied; (b) the ordering of SAMs (TA or MCH) formed under E_{dc} of −0.4 V was worse than under E_{OCP} or E_{dc} of +0.4 and +0.7 V for long (24 h) assembly time. Furthermore, TA-SAMs formed under an E_{dc} of +0.4 V were the most ordered and showed the greatest blocking of $Fe(CN)_6^{3-}$ electron transfer (MCH-SAMs, by comparison, formed under E_{OCP} or E_{dc} of +0.4 and +0.7 V presented almost identical ordering); and (c) both TA and MCH had slow self-assembly dynamics in either the presence or absence of E_{dc}. Finally, achieving the adsorption equilibrium of thiols on gold required a long time (> 24 h) for TA-SAMs under E_{dc} (+0.4 V) and for MCH-SAMs under E_{OCP}.

Experimental results for TA-SAMs showed that the ordering of TA-SAMs was ranked according to the series E_{dc} (+0.4 V) > E_{OCP} > E_{dc} (+0.7 V) > E_{dc} (−0.4 V). Diao et al. [24] studied self-assembly of $HS(CH_2)_{11}CH_3$ ($C_{12}SH$) on gold with ethanol as solvent and also obtained the most ordered SAMs under an E_{dc} of +0.4 V. The authors explained that increasing E_{dc} improved surface adsorption of $C_{12}SH$ for E_{dc} < +0.4 V and desorption of $C_{12}SH$ appeared at E_{dc} > +0.6 V [24]. Other reports indicated that the chemisorption of thiols and the ordering of SAMs would be negatively impacted at negative potentials [13,22], while thiols would easily desorb from the gold surface [20]. It could be imagined that TA was unstable under E_{dc} of −0.4 or +0.7 V, values that were close to the desorption potential of TA on gold (Figure S2, supporting information). Therefore, the poor quality of TA-SAMs formed under E_{dc} either −0.4 or +0.7 V was likely attributed to the desorption of TA from the gold surface. Furthermore, our experiment (Figure 4) showed that C and $\Phi_{1\ Hz}$ were almost the same for TA-SAMs formed under E_{dc} (+0.4 V) or E_{OCP}, whereas Δi and R_{ct} presented the big difference under these conditions. This phenomenon is not likely to be due to desorption of TA because of the almost identical C and $\Phi_{1\ Hz}$ values. We also considered that surface transformation of the TA conformation or composition induced by E_{dc}, which would alter the size and amount of defect sites in TA-SAMs or the surface arrangement of the terminal $-COO^-$ groups of TA-SAMs, possibly led to the difference in $Fe(CN)_6^{3-}$ electron transfer [65–67].

Experimental results showed that the negative potential E_{dc} (−0.4 V) did not improve the ordering of MCH-SAMs. This was ascribed to the instability and desorption of MCH because E_{dc} (−0.4 V) was close to the desorption potential of MCH from gold (Figure S2, supporting information). Unlike TA-SAMs, the ordering of MCH-SAMs formed under E_{dc} (+0.7 V) was similar to those under E_{OCP} and E_{dc} (+0.4 V) because MCH-SAMs were more stable and the desorption of MCH from gold occurred at +1.0 V, a potential larger than that for TA (+0.9 V).

A significant amount of literature reports that applying positive potentials could accelerate the adsorption and ordering of long-chain thiols on gold to obtain defect-free SAMs in a shorter time (generally several minutes) [13–16]. However, our experiments demonstrated that the ordering of short-chain SAMs (TA and MCH) needed a long assembly time in the presence or absence of applied potential. As far as we know, the self-assembly of short-chain thiols under E_{dc} was only studied by a few groups [28,35,46]. A report from van Bennekom et al. detailed the self-assembly of TA on gold in thiol phosphate buffer solution and found that TA-SAMs formed under E_{dc} of either 0 or 0.2 V were more ordered than under E_{OCP} for overnight assembly [35]. Rubinstein et al. reported that $HS(CH_2)_7CH_3$-SAMs (C_8SH) (formed by the method of 1 h C_8SH adsorption with a single electrochemical cycle in H_2SO_4 solution followed by 20 h C_8SH adsorption) had better blocking properties than that made by only 20 h C_8SH adsorption [46]. The above two reports compared the characteristics of thiol SAMs made with long assembly time, but whether potential control could accelerate and obtain stable short-chain SAMs in a shorter time (several minutes) was not clear. Recently, Subramanian et al. reported that the ordering of short-chain $HS(CH_2)_{n-1}CH_3$-SAMs (C_nSH, n = 4, 6 and 8) assembled under E_{dc} (−0.1 V) for short time (20 min) in thiol-containing NaOH aqueous solution was much better than that under E_{OCP} for 12 h in thiol-containing ethanol solution [28]. However, the assembly solvents adopted by Subramanian under E_{dc} (−0.1 V) and E_{OCP} were different. Therefore, it was questionable that the accelerated ordering of short-chain alkanethiols was due to the applied potential. As reported, the ordering of alkanethiol SAMs was the result of a competition between intermolecular interactions of the alkanethiols and the sulfur-gold interactions [68,69]. For long-chain alkanethiols, intermolecular interactions dominated and assisted the formation of closely packed surface structures; for short-chain alkanethiols, sulfur-gold interactions dominated and determined the more tilted packing of thiols on gold [68,69]. Our experiment showed that formation of stable short-chain SAMs under E_{dc} needed much longer time for assembly than long-chain thiols. We considered that mutual interactions (van der Waals forces, electrostatic forces and hydrogen bonds) [68–71] between adjacent chains of thiols played important roles for fast ordering of SAMs in the presence of E_{dc}.

3.6. Exploration of the effect of chain length on the characteristics of SAMs from the literature

In order to further understand the effect of E_{dc} on self-assembly of short-chain and long-chain thiols, we summarized and compared the electrochemical parameters (C, $\Phi_{1\ Hz}$, Δi and R_{ct}) of thiol SAMs with different chain length (n) from literature reports (Table S2–5, supporting information).

Figure 6A shows the plots of C against n for thiol SAMs. As can be seen, C decreased with the increase in n of the thiols. This relationship of C^{-1} with n was linear with the equation $C^{-1} = -0.134 + 6.34 \times 10^{-2}\ n$ ($R^2 = 0.929$), consistent with the linear relationship of $C^{-1} \sim n$ from Helmholtz capacitor equation [48,58]. However, this did not indicate that thiol SAMs could be considered as pure capacitors independent of n. The bigger error bars of C for $n \leq 6$ indicated that short-chain SAMs were easily influenced by their surroundings, such as ion and solvent molecule permeation. For example, Porter reported that plots of C^{-1} (C_nSH-SAMs) with n deviated from the linear relation for a pure capacitor for n < 10 due to ion permeation [58].

Similarly, $\Phi_{1\ Hz}$ reported from literature studies also showed that ions were easier to permeate into short-chain SAMs than into

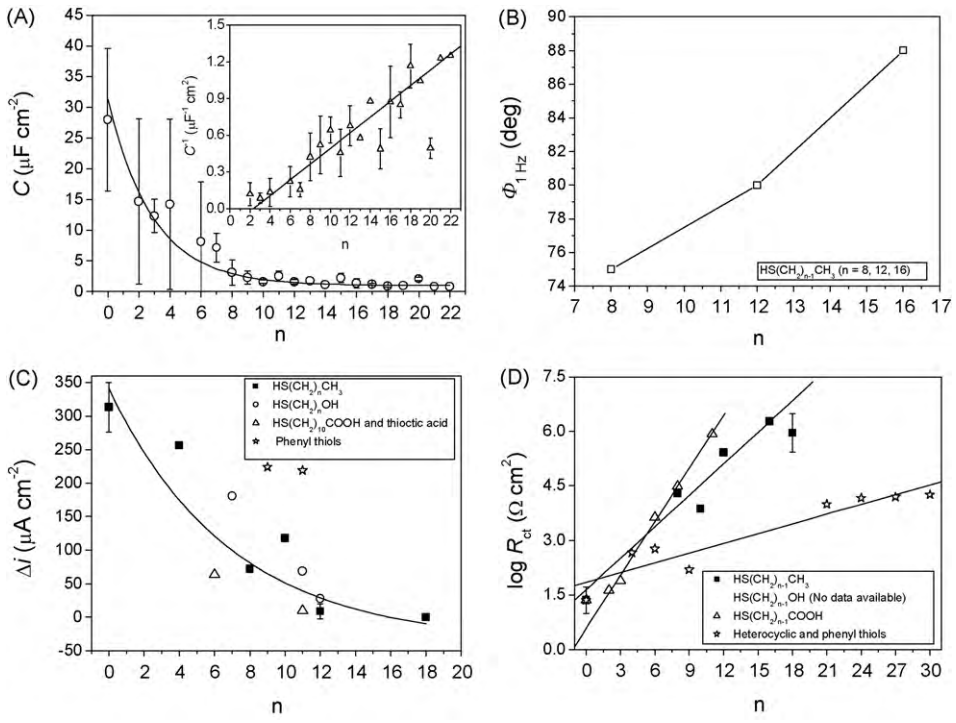

Fig. 6. The plots of electrochemical parameters (A, C; B, $\Phi_{1\ Hz}$; C, Δi; D, logR_{ct}) of bare gold and thiol SAMs in relation to n, according to data from references (Table S2-5, supporting information). Bare Au, n = 0; thiols, n was the quantitative sum of units (e.g. $-CH_2-$, $-CF_2-$, $-C=C-$, $-OH$ and $-CH_3$) of thiol SAMs in the perpendicular direction against Au surface. Inset of Figure 6A is the linear equation of C^{-1} and n; $\Phi_{1\ Hz}$ (Figure 6B) was measured with a potential of −0.34 V; Both Δi and logR_{ct} (Figures 6C and 6D) were the electrochemical responses of $Fe(CN)_6^{3-/4-}$ (total concentration of $Fe(CN)_6^{3-}$ with $Fe(CN)_6^{4-}$ was 1 mM for Δi and 2 mM for logR_{ct} as Table S4 and S5 show). The data in Figure 6 were the average values for the sample number (≥ 3) with the relative standard deviation (RSD) as error bars or the average values for sample number (2).

longer-chain SAMs [50,53]. Figure 6B illustrates that short-chain alkylthiol SAMs resisted ion permeation much more poorly than longer-chain SAMs in 0.05 M K_2HPO_4 (pH = 7). Additionally, $\Phi_{1\ Hz}$ deviated from 88° more significantly at more negative potentials [53].

Figure 6C and D show the plots of Δi and logR_{ct} of $Fe(CN)_6^{3-/4-}$ with n. As can be seen, Δi decreased and logR_{ct} increased with an increase in n. From Figure 6C and D, we could not obviously observe the difference in $Fe(CN)_6^{3-/4-}$ permeation in short-chain and long-chain SAMs because Δi and logR_{ct} were related to not only the defects in the SAMs, but also the distance (thickness of thiol SAMs) between probes and the electrode surface. Systematic investigation of electron transfer through C_nSH-SAMs (n = 2 ~ 18) on gold by Offenhausser [72] using ferrocenecarboxylic acid (FA) as the redox probe showed that the oxidation peak current of FA in C_nSH-SAMs was almost the same as on bare Au for $n \leq 6$, then decreased significantly for $n \geq 8$. Experiments from other groups also observed almost the same electrochemical responses for redox probes in short-chain SAMs ($n \leq 6$) and on bare Au [47,48,73]. These results indicated that a lot of defects existed in SAMs for $n \leq 6$, which favored the permeation of redox probes into the SAM structure.

Other techniques, such as infrared spectroscopy (IR), ellipsometry and scanning tunneling microscopy (STM), also proved that short-chain SAMs were more loosely-packed and defective than long-chain SAMs, making them more susceptible to ion and solvent permeation [28,48,58,65,74–77]. As reported, ion and solvent molecule permeation could induce the formation of defects, especially in short-chain SAMs [53,78,79]. The time needed to heal these defects in short-chain SAMs was found to be longer when compared with long-chain SAMs. Therefore, permeation of ions and solvent molecules in SAMs likely dominated the slow self-assembly dynamics of short-chain thiols (TA and MCH) on gold. This observation also emphasized the significance of mutual interactions between adjacent chains of thiols on the fast ordering of SAMs in the presence of E_{dc}.

4. Conclusion

Self-assembly of short-chain thiols (TA and MCH) under E_{OCP} and E_{dc} (−0.4, +0.4 and +0.7 V) was investigated in this article based on the electrochemical parameters C, $\Phi_{1\ Hz}$, Δi and R_{ct}, analyzed by *CV* and *EIS*. The main conclusions were as follows: (1) Potential control for short time (30 min) assembly could not obtain more stable SAMs. Both TA and MCH had slow self-assembly dynamics and needed a long time (> 24 h) to arrive at the adsorption equilibrium; (2) the negative potential E_{dc} (−0.4 V) did not improve the ordering of SAMs. The ordering of TA-SAMs was the best when assembled under E_{dc} (+0.4 V), whereas the ordering of MCH-SAMs was almost the same when assembled under either E_{OCP} or E_{dc} (+0.4, +0.7 V); and (3) compared with long-chain thiols, which could form defect-free SAMs in a short time (generally several minutes) under E_{dc}, we suspected that permeation of ions and water molecules dominated the slow self-assembly dynamics of short-chain thiols and that mutual interactions between adjacent chains of thiols played an important role in the fast ordering of SAMs in the presence of E_{dc}. The merit of this work was that *CV* and *EIS* were crosschecked and could be used for conveniently judging the validity of experimental data and discussing the dynamics of ion permeation and electron transfer through thiol SAMs. The internal relationships of the parameters C, $\Phi_{1\ Hz}$, Δi and R_{ct} obtained by us, together with the data summarized from the literature (Table S2-5, supporting information), provide a valuable reference for scientists studying electrochemical sensors with thiol SAMs.

Acknowledgments

This work was supported by the NSFC (Nos. 20975049 & 20575025), State Key Laboratory of Electrochemistry of China at the Changchun Applied Chemistry Institute (2008008) and the Analytical Center of Nanjing University. The authors acknowledge the reviewers for their valuable suggestions.

Appendix A. Supplementary data

Supplementary data associated with this article can be found, in the online version, at doi:10.1016/j.electacta.2010.05.028.

References

[1] J.C. Love, L.A. Estroff, J.K. Kriebel, R.G. Nuzzo, G.M. Whitesides, Chem. Rev. 105 (2005) 1103.
[2] R.L. Millen, J. Nordling, H.A. Bullen, M.D. Porter, Anal. Chem. 80 (2008) 7940.
[3] J.J. Gooding, F. Mearns, W.R. Yang, J.Q. Liu, Electroanalysis 15 (2003) 81.
[4] J.Y. Dai, Z.G. Li, J. Jin, Y.Q. Shi, J.J. Cheng, J. Kong, S.P. Bi, Biosens. Bioelectron. 24 (2009) 1074.
[5] F. Schreiber, Prog. Surf. Sci. 65 (2000) 151.
[6] J.Y. Dai, Z.G. Li, J. Jin, J.J. Cheng, J. Kong, S.P. Bi, J. Electroanal. Chem. 624 (2008) 315.
[7] J.Y. Dai, J.J. Cheng, Z.G. Li, Y.Q. Shi, N. An, S.P. Bi, Electrochem. Commun. 10 (2008) 582.
[8] J.Y. Dai, J.J. Cheng, J. Jin, Z.G. Li, J. Kong, S.P. Bi, Electrochem. Commun. 10 (2008) 587.
[9] J.Y. Dai, J.J. Cheng, Z.G. Li, J. Jin, S.P. Bi, Electrochim. Acta 53 (2008) 3479.
[10] J.J. Cheng, J.Y. Dai, J. Jin, L. Qiu, G.Y. Fang, Z.G. Li, Y.B. Sun, S.P. Bi, Thin Solid Films 517 (2009) 3661.
[11] D. Qu, M. Morin, J. Electroanal. Chem. 565 (2004) 235.
[12] D. Qu, M. Morin, J. Electroanal. Chem. 524 (2002) 77.
[13] M. Rohwerder, K. de Weldige, M. Stratmann, J. Solid State Electrochem. 2 (1998) 88.
[14] F.Y. Ma, R.B. Lennox, Langmuir 16 (2000) 6188.
[15] C.M.A. Brett, S. Kresak, T. Hianik, A.M.O. Brett, Electroanalysis 15 (2003) 557.
[16] Z. Petrovic, M. Metiko-Hukovic, R. Babic, J. Electroanal. Chem. 623 (2008) 54.
[17] D.E. Weisshaar, B.D. Lamp, M.D. Porter, J. Am. Chem. Soc. 114 (1992) 5860.
[18] K. de Weldige, M. Rohwerder, E. Vago, H. Viefhaus, M. Stratmann, Fresenius J. Anal. Chem. 353 (1995) 329.
[19] C. Frubose, K. Doblhofer, J. Chem. Soc. Faraday Trans. 91 (1995) 1949.
[20] M. Riepl, V.M. Mirsky, O.S. Wolfbeis, Mikrochim. Acta 131 (1999) 29.
[21] J. Wang, M. Jiang, A.M. Kawde, R. Polsky, Langmuir 16 (2000) 9687.
[22] L. Cheng, J.P. Yang, Y.X. Yao, D.W. Price, S.M. Dirk, J.M. Tour, Langmuir 20 (2004) 1335.
[23] N.K. Devaraj, P.H. Dinolfo, C.E.D. Chidsey, J.P. Collman, J. Am. Chem. Soc. 128 (2006) 1794.
[24] P. Diao, Q.C. Hou, M. Guo, M. Xiang, Q. Zhang, J. Electroanal. Chem. 597 (2006) 103.
[25] W.K. Paik, S. Eu, K. Lee, S. Chon, M. Kim, Langmuir 16 (2000) 10198.
[26] S. Chon, W.K. Paik, Phys. Chem. Chem. Phys. 3 (2001) 3405.
[27] S. Bengio, M. Fonticelli, G. Benitez, A.H. Creus, P. Carro, H. Ascolani, G. Zampieri, B. Blum, R.C. Salvarezza, J. Phys. Chem. B 109 (2005) 23450.
[28] S. Subramanian, S. Sampath, Anal. Bioanal. Chem. 388 (2007) 135.
[29] Y. Han, K. Uosaki, Electrochim. Acta 53 (2008) 6196.
[30] R. Zugle, J. Kambo-Dorsa, P.Y. Gadzekpo, Talanta 61 (2003) 837.
[31] D. Burshtain, D. Mandler, J. Electroanal. Chem. 581 (2005) 310.
[32] S. Zhang, C.M. Cardona, L. Echegoyen, Chem. Commun. 43 (2006) 4461.
[33] K. Ariga, T. Nakanishi, T. Michinobu, J. Nanosci. Nanotech. 6 (2006) 2278.
[34] G.K. Olivier, D. Shin, J.B. Gilbert, L.M.A. Monzon, J. Frechette, Langmuir 25 (2009) 2159.
[35] M. Dijksma, B. Kamp, J.C. Hoogvliet, W.P. van, Bennekom, Langmuir 16 (2000) 3852.
[36] R.K. Shervedani, S.A. Mozaffari, Anal. Chem. 78 (2006) 4957.
[38] Q.J. Chi, J.D. Zhang, J. Ulstrup, J. Phys. Chem. B 110 (2006) 1102.
[39] M.H. Schoenfisch, J.E. Pemberton, Langmuir 15 (1999) 509.
[40] G. Benitez, C. Vericat, S. Tanco, F.R. Lenicov, M.F. Castez, M.E. Vela, R.C. Salvarezza, Langmuir 20 (2004) 5030.
[41] A. Kudelski, Langmuir 19 (2003) 3805.
[42] G. Nelles, H. Schonherr, M. Jaschke, H. Wolf, M. Schaub, J. Kuther, W. Tremel, E. Bamberg, H. Ringsdorf, H.J. Butt, Langmuir 14 (1998) 808.
[43] R. Desikan, S. Armel, H.M. Meyer, T. Thundat, Nanotechnology 18 (2007) 424028.
[44] Q.M. Xu, L.J. Wan, C. Wang, C.L. Bai, Z.Y. Wang, T. Nozawa, Langmuir 17 (2001) 6203.
[45] S. Campuzano, R. Galvez, M. Pedero, F.J.M. de Villena, J.M. Pingarron, J. Electroanal. Chem. 526 (2002) 92.
[46] M. Wanunu, A. Vaskevich, I. Rubinstein, Israel J. Chem. 45 (2005) 337.
[47] Q. Cheng, A. Brajter-Toth, Anal. Chem. 64 (1992) 1998.
[48] Q. Cheng, A. Brajter-Toth, Anal. Chem. 67 (1995) 2767.
[49] V. Ganesh, S.K. Pal, S. Kumar, V. Lakshminarayanan, Electrochim. Acta 52 (2007) 2987.
[50] V. Ganesh, V. Lakshminarayanan, Langmuir 22 (2006) 1561.
[51] E. Boubour, R.B. Lennox, Langmuir 16 (2000) 4222.
[52] E. Boubour, R.B. Lennox, Langmuir 16 (2000) 7464.
[53] E. Boubour, R.B. Lennox, J. Phys. Chem. B 104 (2000) 9004.
[54] Y.F. Xing, S.J. O'Shea, S.F.Y. Li, J. Electroanal. Chem. 542 (2003) 7.
[55] C. Miller, P. Cuendet, M. Graetzel, J. Phys. Chem. 95 (1991) 877.
[56] M. Dijksma, B.A. Boukamp, B. Kamp, W.P. van, Bennekom, Langmuir 18 (2002) 3105.
[57] W. Limbut, P. Kanatharana, B. Mattiasson, P. Asawatreratanakul, P. Thavarungkul, Biosens. Bioelectron. 22 (2006) 233.
[58] M.D. Porter, T.B. Bright, D.L. Allara, C.E.D. Chidsey, J. Am. Chem. Soc. 109 (1987) 3559.
[59] P. Diao, D.L. Jiang, X.L. Cui, D.P. Gu, R.T. Tong, B. Zhong, J. Electroanal. Chem. 464 (1999) 61.
[60] H.O. Finklea, D.A. Snider, J. Fedyk, E. Sabatani, Y. Gafni, I. Rubinstein, Langmuir 9 (1993) 3660.
[61] X.Q. Lu, H.Q. Yuan, G.F. Zuo, J.D. Yang, Thin Solid Films 516 (2008) 6476.
[62] D. García-Raya, R. Madueno, J.M. Sevilla, M. Blázquez, T. Pineda, Electrochim. Acta 53 (2008) 8026.
[63] Y. Wang, A.E. Kaifer, J. Phys. Chem. B 102 (1998) 9922.
[64] V. Dharuman, J.H. Hahn, Sens. Actuators B 127 (2007) 536.
[65] Y.F. Liu, Y.C. Yang, Y.L. Lee, Nanotechnology 19 (2008) 065609.
[66] R.L. Garrell, J.E. Chadwick, D.L. Severance, N.A. MConald, D.C. Myles, J. Am. Chem. Soc. 117 (1995) 11563.
[67] M.J. Tarlov, D.R.F. Burgess, G. Gillen, J. Am. Chem. Soc. 115 (1993) 5305.
[68] E. Barrena, E. Palacios-Lidon, C. Munuera, X. Torrelles, S. Ferrer, U. Jonas, M. Salmeron, C. Ocal, J. Am. Chem. Soc. 126 (2004) 385.
[69] A. Cossaro, R. Mazzarello, R. Rousseau, L. Casalis, A. Verdini, A. Kohlmeyer, L. Floreano, S. Scandolo, A. Morgante, M.L. Klein, G. Scoles, Science 321 (2008) 943.
[70] E. Ito, K. Konno, J. Noh, K. Kanai, Y. Ouchi, K. Seki, M. Hara, Appl. Surf. Sci. 244 (2005) 584.
[71] U. Tasic, B.S. Day, T.Y. Yan, J.R. Morris, W.L. Hase, J. Phys. Chem. C 112 (2008) 476.
[72] S. Lingler, I. Rubinstein, W. Knoll, A. Offenhausser, Langmuir 13 (1997) 7085.
[73] V.A. Pedrosa, T.R.L.C. Paixao, R.S. Freire, M. Bertotti, J. Electroanal. Chem. 602 (2007) 149.
[74] M.J. Esplandiu, H. Hagenstrom, D.M. Kolb, Langmuir 17 (2001) 828.
[75] S. Campuzano, M. Pedrero, C. Montemayor, E. Fatas, J.M. Pingarron, J. Electroanal. Chem. 586 (2006) 112.
[76] K. Konno, E. Ito, J. Noh, M. Hara, Jpn. J. Appl. Phys. 45 (2006) 405.
[77] Z.G. Hu, P. Prunici, P. Patzner, P. Hess, J. Phys. Chem. B 110 (2006) 14824.
[78] U.K. Sur, V. Lakshminarayanan, J. Electroanal. Chem. 516 (2001) 31.
[79] M.R. Anderson, M.N. Evaniak, M.H. Zhang, Langmuir 12 (1996) 2327.